

Antal Kerpely Doctoral School of Materials Science and Technology



Development of Innovative Thermal Insulation Building Materials Based on Zeolite-Poor Rock and Solid Wastes

Thesis Booklet

By

Jamal Eldin Fadoul Mohammed Ibrahim

Supervisors

Prof. Dr. László A. Gömze †,

Professor Emeritus

Dr. István Kocserha

Associate Professor

Head of the Doctoral School

Prof. Dr. Valéria Mertinger

Institute of Ceramic and Polymer Engineering

Faculty of Material Science and Engineering

University of Miskolc

Miskolc, Hungary

2022

1. Introduction

Energy consumption recently became a global concern due to its environmental and economic impact [1]. It has been reported that an expected 50% increase in overall energy consumption will take place worldwide until the year 2050, while the buildings sector is anticipated to dissipate 40% of the total global energy consumption [2]. Therefore, energy efficiency is becoming a top priority for eco-friendly construction since the building sector is the biggest energy consumer.

Future high-energy-saving buildings can play a crucial role in facing sustainable energy challenges by reducing the contribution of building to climate change, reducing global greenhouse gas emissions, and enhancing energy security and sovereignty [3]. Therefore, minimising energy usage in buildings by using passive techniques such as thermal insulation is of increasing popularity [4]. The walls are the main areas via which significant quantities of heat interchange between the building and the surrounding environment. It is worth mentioning that a large amount of energy consumption in the building is due to heat loss and gain throughout the wall [5].

The fast population growth, urbanisation, industrialisation, and various other human activities lead to a huge release of waste and a great demand for construction materials [6]. Another problem is the fast depletion of natural resources, resulting in scarcity and concerns about the availability of raw materials [7]. Sintered ceramic materials such as bricks and glass-ceramic foams have emerged as a highly promising technical option for recycling solid wastes lately [8]. The growing demand for building materials prompted an urgent search for sustainable alternatives, including natural and waste materials that can be used to synthesise construction materials with superior thermal insulation characteristics. Among natural materials, zeolite-poor rocks and solid waste could be excellent candidates for synthesising construction materials with better thermal insulation [9]. Various scientific studies have been performed on using zeolite-poor rocks in construction as an additive to cement or masonry blocks [10]. Despite many studies on this topic, no research has been conducted to evaluate zeolite-poor rocks together with solid wastes (sawdust and eggshell) as primary raw materials for bricks and glass-ceramic foams production.

The development of novel composite bricks and glass-ceramic foams utilising easily obtainable, low-price raw materials at an economical cost is particularly appealing. This may significantly decrease production costs, increase competitiveness, and minimise environmental concerns by conserving energy, decreasing pollution, and lowering waste disposal expenses.

2. Summary of literature

2.1. Thermal insulation in buildings

Insulation standards for new construction have grown over time in response to rising concerns about indoor air quality, human comfort, and environmental impact. For this reason, there is a great potential for energy savings and for policies to impose energy-efficiency improvements for both new and existing buildings. Among the building materials that offer thermal insulation, porous bricks and glass-ceramic foams are reliable sustainable materials. Lowering the thermal conductivity of building materials is a crucial step in improving thermal insulation in buildings.

One way to do this is by incorporating appropriate additives into the raw materials and/or using new materials. Huge interest has been devoted lately to the development of new thermal insulation materials [11]. Zeolite-poor rock is a potential candidate for the synthesis of porous bricks and glass-ceramic foams with outstanding properties.

2.2. Zeolite-poor rocks

Zeolite-poor rocks are naturally-occurring rocks. They generally have a low zeolite content (less than 10%), besides other minerals like calcite, cristobalite, quartz, montmorillonite, and sometimes feldspar [12]. Their low amount of zeolite limited their advanced capabilities. However, zeolite-poor rocks are good construction materials because of their good mechanical behaviour, excellent porosity, and lightweight. They could be utilised to make porous structural materials with improved thermal insulation characteristics [13].

2.3. Use of zeolitic tuff in the building industry

Despite several research investigations on zeolite-poor rocks, very little research has been done to assess zeolite-poor rocks as raw materials for construction applications. Samardzioska et al. studied the stability of natural zeolite bricks under different laboratory conditions. Kazantseva et al. [14] investigated the usage of natural zeolite as primary raw material to prepare porous ceramics. Tanijaya et al. [15] also examined the potential application of natural zeolite as an additive for concrete production. It's worth noting that zeolite-poor rocks are very cheap and are widely distributed. It can also be a waste product from the separation during screening procedures for manufacturing granulated zeolite-rich rock in quarries. Zeolite-poor rocks can be used together with waste materials to produce new porous ceramic materials.

2.4. Previous studies on recycling waste materials in fired-clay bricks

Waste management is becoming an issue in many countries since untreated waste materials create critical environmental problems. Thus, the inclusion of waste materials in the brick preparation will reduce the massive use of clay resources and contribute to these wastes' safe disposal. Several research works have been reported regarding the inclusion of many waste materials into the clay to produce eco-friendly building bricks. When comparing the findings of this study to those of the literature, it is worth noting that zeolite-poor rock incorporated sawdust and eggshell are promising materials for brick making, as their produced bricks have higher compressive strengths and better insulation properties than many of the studies listed in the literature.

2.5. Glass-ceramic foams

Compared to the other construction materials that provide thermal insulation, glass-ceramic foams are considered the most dependable eco-friendly materials. They compose of a widespread array of pores and are made up of vitreous (amorphous) phase together with crystalline phases [16]. Glass-ceramic foam is a heterogeneous system containing a mixture of gaseous and solid constituents; the solid phase is a glassy phase with micrometre-thick single-cell walls, while the gaseous phase fills the cells.

2.6. The uses of alternative raw materials for producing glass-ceramic foam

The production of glass-ceramic foam would be an energy-consuming process if they made from mixes based on prepared powdered glass or cullet obtained straight from the manufacturing process due to a twofold heating process. Therefore, the topic of employing less expensive raw materials in foams manufacturing has long been raised. Using natural materials and recycling waste glass that is both highly efficient and cost-effective is one of the techniques for resolving this challenge. Recently, various solid wastes, including fly ash [17], tailings wastes [18], incineration ashes [19], red mud, and coal bottom ash waste [20], have been studied as potential materials for the production of glass-ceramic foam. Nevertheless, very limited attention has been given to the utilisation of zeolite-poor rock to manufacture glass-ceramic foams.

2.7. Knowledge gap

To the best of our knowledge, no research has been conducted to investigate zeolite-poor rock incorporated solid waste usage as primary raw materials for preparing porous bricks and glass-ceramic foams. Based on the literature, The possibility of using solid waste (sawdust and eggshell) as pore-forming agents in zeolite-poor rock samples needs to be examined. Furthermore, mechanical milling and the optimal condition for the compaction process of zeolite-poor rocks containing sawdust and eggshell need to be investigated. In addition, the effect of alkali activation, composition and sintering temperature on the technical properties of the produced new porous bricks and glass-ceramic foams are worth studying.

3. Materials and Methods

3.1 Materials

Zeolite-poor rock was utilised as the primary raw material in this investigation. It was obtained from mining in Mád (Tokaj region). Zeolite-poor rock was collected as granules after quarrying and pre-crushing. Sawdust was collected as waste material from local areas and sieved to pass a 200 μm gyratory sieve. Hen's eggshell was obtained as waste and ground to powder. Sodium hydroxide was purchased from Donauchem GmbH (Hungary) in the form of a granule.

3.2. Preparation methods

3.3.1. Preparation of zeolite-poor rock incorporated sawdust and eggshell composite bricks

Fig 1 shows a manufacturing diagram with the essential steps involved in making burnt zeolite-poor rock incorporated sawdust and eggshell composite bricks. Several proportions of sawdust and eggshell (Table. 1) have been selected and uniformly blended and milled with zeolite-poor rock using PM 400 Retsch planetary ball mill for 15 minutes run at 200 rpm to produce homogenous mixtures (zeolite-poor rock containing sawdust and zeolite poor rock containing eggshell). The produced dry mixtures were then uniaxially compacted to form cylindrical composite bricks with a thickness of roughly 10 mm and a diameter of 25 mm using a pressure of 40-45 MPa. The compacted samples were then sintered in a laboratory-scale electrical kiln

at various temperature ranges (950, 1050, 1150 and 1250 °C) for 2 h at a rate of 60 °C/h to acquire the desired strength.

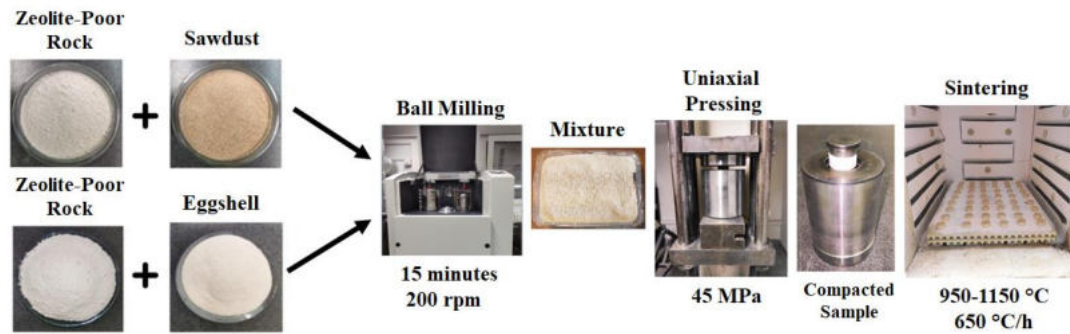


Figure 1. Processing steps of the zeolite-poor rock containing sawdust and eggshell composite ceramic bricks

Table 1. Mixture proportions of the raw materials for porous bricks making

Mix code	Zeolite-poor rock (wt%)	Sawdust (wt%)	Mix code	Zeolite-poor rock (wt%)	Eggshell (wt%)
Z	100	0	Z	100	0
ZS2	98	2	ZE5	95	5
ZS4	96	4	ZE10	90	10
ZS6	94	6	ZE15	85	15
ZS8	92	8	ZE20	80	20
ZS10	90	10			

3.3.1. Preparation of zeolite-poor rock incorporated sawdust and eggshell foams

Zeolite-poor rock combined with sawdust and eggshell foams were synthesised using the alkali activation and reactive sintering technique (Fig. 2). Crushed zeolite-poor rock powders were mixed with different proportions of sawdust and eggshell (Table.2), 15 wt% of NaOH granules were dissolved in distilled water and added to the previously prepared zeolite poor rock with sawdust and zeolite poor rock with eggshell mixtures, an exothermic reaction took place associated with evolving of heat and bubbles. The mixtures were then dried in the oven for two days at 200 °C. The alkali-activated mixtures were ground in a planetary ball mill (Retsch) at 150 rpm for 15 minutes. Then, the produced powders were uniaxially compacted into pellets at 18 MPa with an initial height of 10 mm and a diameter of 20 mm. The prepared green specimens were then sintered at 850-950 °C for 10 min using a laboratory electric kiln.

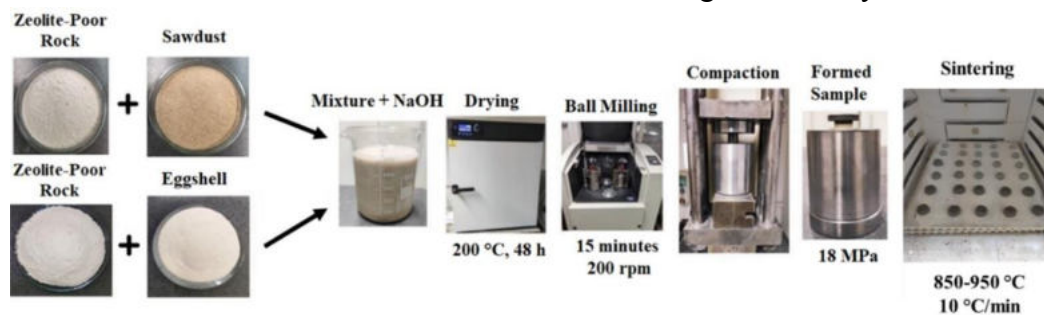


Figure 2. Preparation steps of alkali-activated zeolite-poor rock incorporated eggshell foams

Table 2. Mix proportion in wt (%) of the raw materials

Designation of the mixtures	Prepared mixture composition			Designation of the mixtures	Prepared mixture composition		
	Zeolite-poor rock (wt%)	Sawdust (wt%)	Sodium hydroxide (wt%)		Zeolite-poor rock (wt%)	Sawdust (wt%)	Sodium hydroxide (wt%)
ZS	100	0	15	ZS	100	0	15
Z2SS	98	2	15	Z2SS	98	2	15
Z4SS	96	4	15	Z4SS	96	4	15
Z6SS	94	6	15	Z6SS	94	6	15
Z8SS	92	8	15	Z8SS	92	8	15
Z10SS	90	10	15	Z10SS	90	10	15
Z20SS	80	20	15	Z20SS	80	20	15

3.3 Testing methods

The particle size distributions of milled powders were investigated by a laser particle size distribution analyser, while the specific surface area was estimated based on the Brunauer-Emmett-Teller method using a Micromeritics Tristar 3000 instrument. Rigaku Miniflex II X-ray diffractometer was used to investigate the raw materials' mineralogical and phase composition at room temperature. The diffractometer is operated in Bragg-Brentano geometry, using $\text{CuK}\alpha$ radiation at a wavelength of $\lambda = 1.5418 \text{ \AA}$. The scanning of the samples was carried out in a 2θ range of (4–90 °) using a scanning speed of 1°/min while the step size was 0.01015 °. The thermal properties, involving parallel differential and thermogravimetric analyses, were assessed via a thermal analyser (1750 SETARAM, Sestys evolution) operating at a 10 °C/min heating rate in a steady oxygen environment throughout a temperature range of 38–1200 °C. The raw materials powders' topographical features and morphological characteristics were analysed using two scanning electron microscopies (SEM, Carl Zeiss EVO MA10, and Thermo Helios G4-PFIB CXe Dual-Beam), fitted with a Bruker microprobe, and running at a voltage of 20 kV. Before SEM imaging, the raw powders and the fractured samples were coated with multi-layers of gold, utilising coating spray devices to enhance conductivity. The photos were captured under different magnifications using ES-BSD mode. An energy-dispersive X-ray spectrometer (EDAX Genesis and EDAX Octane Elect-Plus) was used to provide quantitative and qualitative analyses of the elemental composition of the samples. The foaming tendencies and the optimal sintering temperatures of the alkali-activated samples were carried out using a Camar Elettronica heating microscope operated with a 5 °C/min heating rate. The samples' infrared (IR) spectra were captured via a Bruker Tensor 27 FTIR (Fourier transform infrared spectroscopy) equipment. The functional group's analysis was performed on all samples using the transmittance technique.

4. Results and discussion

4.1. Raw materials analysis

4.1.1. Particle size distribution of the raw materials

The particle size distribution curves (Fig. 3) demonstrate that zeolite-poor rock has a larger percentage of smaller particles, whereas sawdust has a high percentage of a coarser fraction.

The average sizes for zeolite-poor rock, sawdust and eggshell (D50) were 16.61 μm , 71.2 μm , and 25.49 μm , respectively.

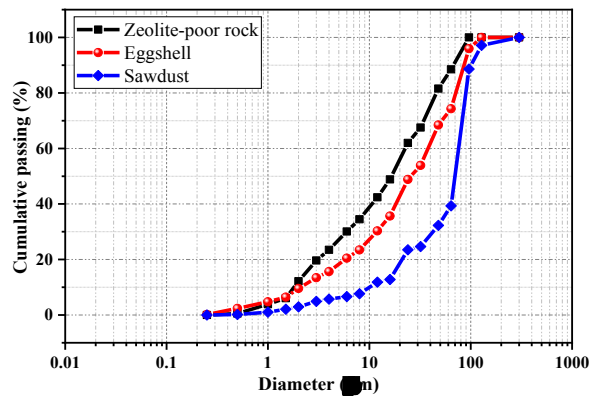


Figure 3. Particle-size distribution of the zeolite-poor rock, sawdust and eggshell

4.1.2. XRD and XRF examinations of the raw materials

The XRD analysis of the raw materials is shown in Fig. 4. Zeolite-poor rock from Tokaj region (Hungary) contains clinoptilolite together with other mineral phases, including montmorillonite, quartz, cristobalite, and calcite, as confirmed by XRD measurement (Fig. 4.a). Fig 4.b depicts the XRD diffractogram of sawdust. The result shows two diffraction peaks at corresponding 2θ values of 15.6° and 22.4° , which are designated to the crystallographic planes of (101) and (002) of cellulose I. The XRD analysis of the eggshell is shown in Fig. 4.c. The occurrence of calcite with rhombohedral structure was confirmed as the fundamental component of the eggshell.

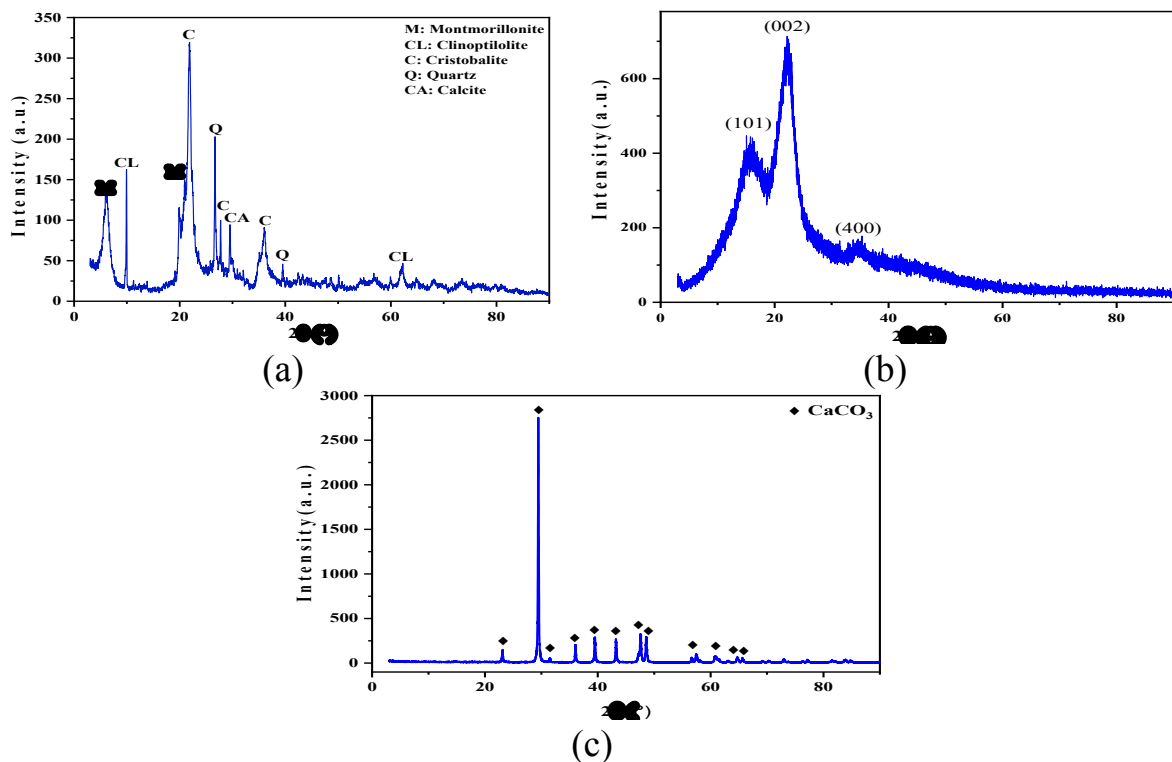


Figure 4. XRD patterns of a) zeolite-poor rock, b) sawdust and c) eggshell

4.2. Results of the new zeolite-poor rock incorporated sawdust composite bricks

4.2.1. Dimensional characteristic of zeolite-poor rock/sawdust bricks after firing

Cylindrical zeolite-poor rock bricks incorporated with different percentages of sawdust are manufactured using variable sintering temperatures (Fig. 5). The produced samples are fired into interesting white-like colours with noticeable volume shrinkage.



Figure 5. Laboratory-scale zeolite-poor rock/sawdust ceramic bricks sintered at different temperatures

4.2.2. SEM examination of the fired zeolite-poor rock/sawdust bricks

Fig. 6 shows different magnifications of the fracture surface of ceramic bricks containing 8% sawdust sintered at 1150 °C. The SEM images show different types of pores (open, closed, and capillaries) of different sizes. At high magnification, a whisker-like structure can be seen, which is confirmed to be mullite.

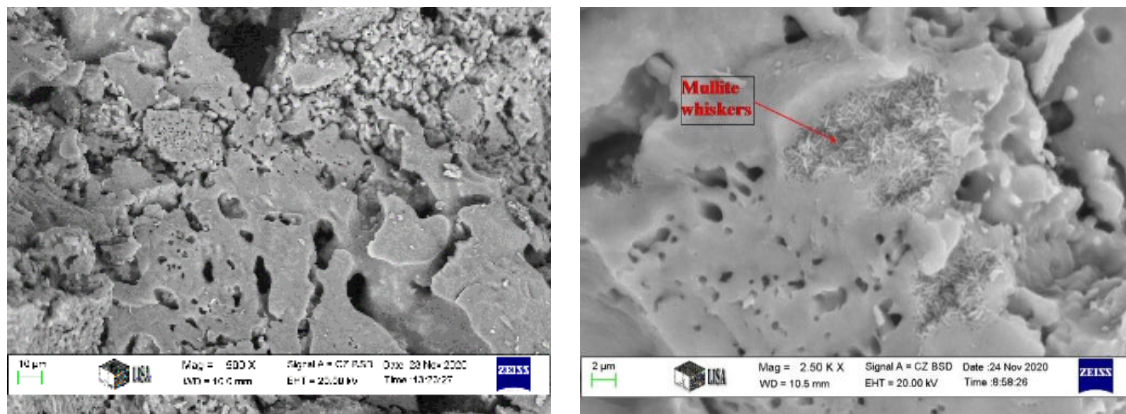


Figure 6. SEM images with different magnifications of the fracture surface of ZS8 sintered at 1150 °C

4.2.3. Technical properties of the fired zeolite-poor rock/sawdust bricks

Upon increasing the sintering temperature, the sawdust tends to decompose and produce carbon dioxide, which is emitted from the sample producing different types of pores (close, open and capillaries). Therefore, the porosity increases while the density decreases (Fig. 7). The increase in porosity leads to a decrease in thermal conductivity of the samples. Thermal conductivity is well known to be connected to porosity since the open pores are usually filled with air, acting as an insulator and reducing thermal conductivity. The inclusion of sawdust in the zeolite-poor

rock reduces the compressive strength in all sintering temperatures. In this work, all the produced bricks show compressive strength above 7 MPa, except the samples that contain 10% sawdust fired at 950 °C, which offers a compressive strength of 4 MPa. Therefore, these bricks are suitable for construction applications.

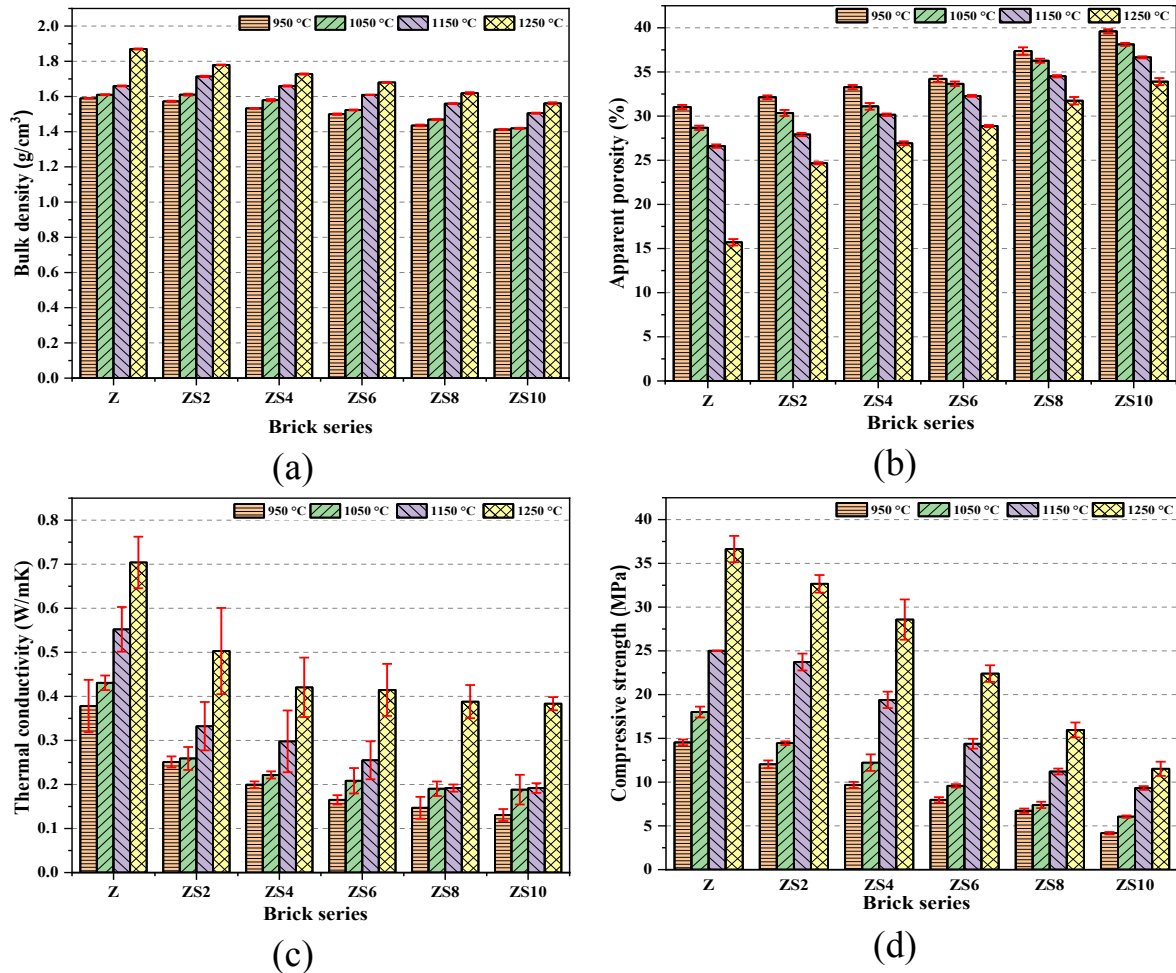


Figure 7. The correlation between a) density, b) apparent porosity c) thermal conductivity, d) and sawdust content of the samples sintered at different temperatures

4.3. Result of innovative composite bricks based on zeolite-poor rock and hen's eggshell

4.3.1. Dimensional properties of fired zeolite-poor rock/eggshell bricks

The zeolite-poor rock bodies could sustain the addition of eggshell powder in different percentages, as can be seen in the produced composite bricks heat-treated at variable temperatures (Fig. 8). With increasing the firing temperature, variations in the colours of the sintered bricks were noticed. The key alterations that the samples underwent throughout the heat treatment process were decomposition and phase transformation accompanied by volume shrinkage. The produced zeolite-based composite bricks have excellent surface finishing, which can be used as facing bricks.

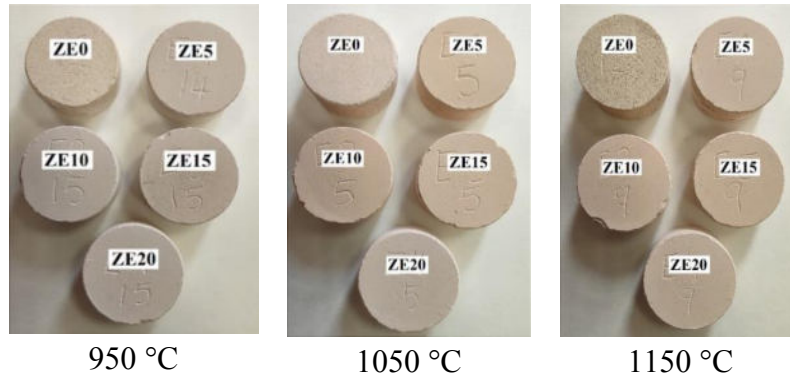


Figure 8. Prototype zeolite-poor rock/eggshell ceramic bricks sintered at variable temperatures

4.3.2. Technical properties of the fired zeolite-poor rock/eggshell bricks

The bulk density of the samples from all groups indicated a gradual decrease with increasing eggshell. This could be due to the fact that at 900 °C, vitrification will take place associated with CO₂ emission resulting from the decomposition of calcite contained in raw materials (zeolite-poor rock and eggshell), part of the gas will be released, making open pores and capillaries in the brick body while the viscous phase holds part of the gas inside making closed pores, the higher amount of eggshell release a larger amount of CO₂ which resulted in higher porosity and low density of the samples. The higher porosity resulted in low thermal conductivity and compressive strength (Fig. 9).

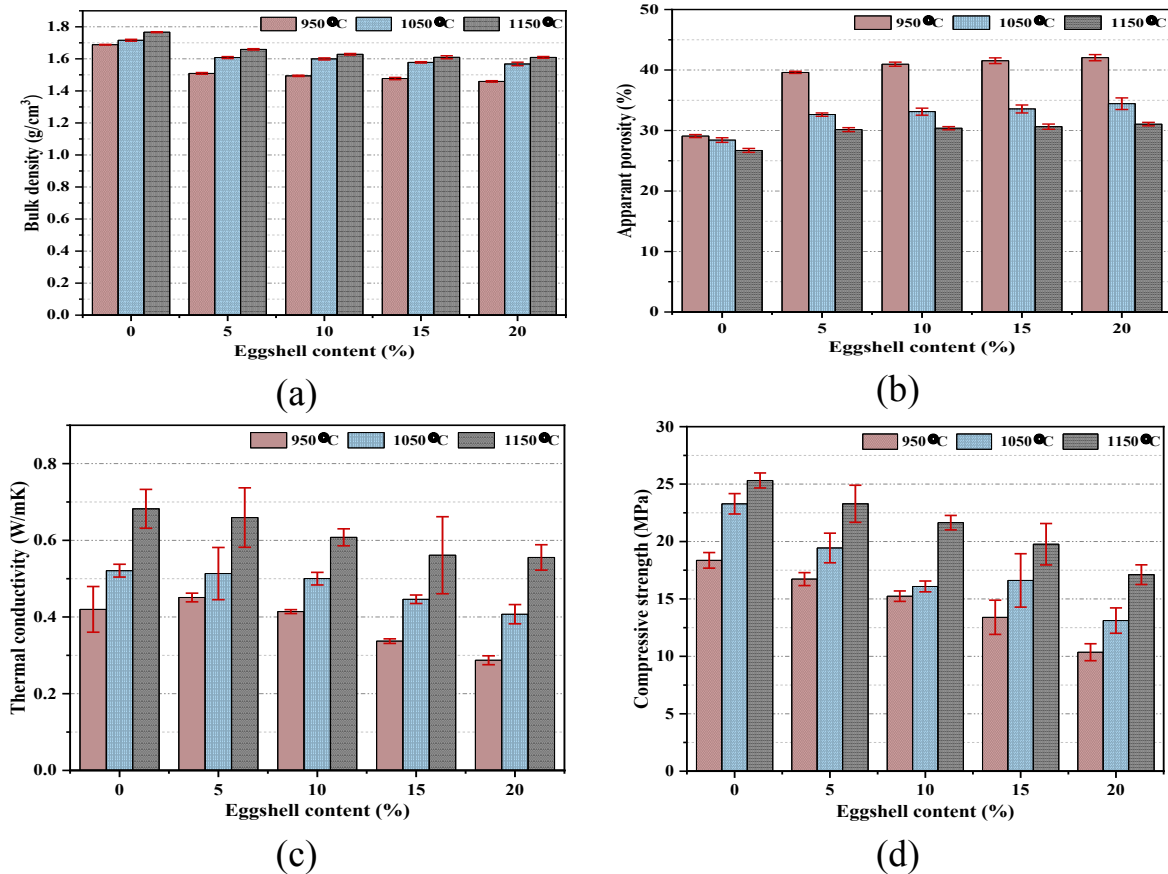


Figure 9. The correlation between a) density, b) apparent porosity c) thermal conductivity, d) and eggshell content of the samples sintered at different temperatures

4.4. Result of alkali-activated zeolite-poor rock incorporated sawdust glass-ceramic foams

4.4.1. Dimensional properties of the sintered zeolite-poor rock/sawdust foams

Fig. 10 depicts the produced glass-ceramic foams' macrostructures and morphology. It is worth mentioning that increasing the sawdust content and sintering temperature increases pore size, porosity, and overall volume expansion. Due to the fact that adding more sawdust produces more gas and raising the temperature produces viscous material coupled with greater internal gas pressure, the pores rapidly expanded owing to the coalescence of tiny pores. The most important point to emphasise is that a portion of the sawdust gets converted through the reduction sintering to carbon and deposited on the foam's inside surface, resulting in black colouration.

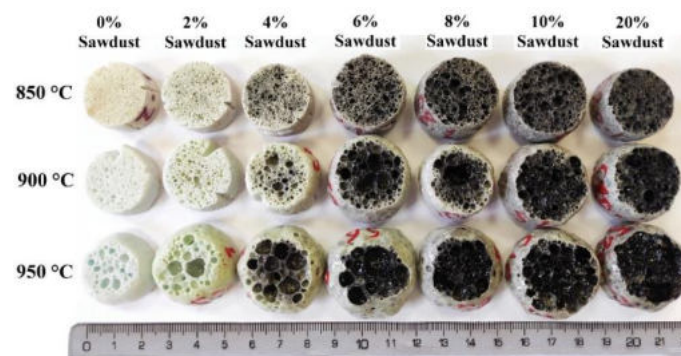


Figure 10. The produced foams with different sawdust contents sintered at different temperatures

4.4.2. XRD investigations of the sintered zeolite-poor rock/sawdust foams

Fig. 11 exhibits the XRD spectra of zeolite-poor rock powder, alkali-activated Z6SS mixture, and Z6SS glass-ceramic foams heat-treated under different sintering temperatures. The XRD of the alkali-activated sample confirms the chemical reaction of cristobalite, quartz, montmorillonite, clinoptilolite, and calcite with sodium hydroxide and the formation of heulandite. Upon the sintering and at 850 °C, the decomposition of heulandite has taken place and formation of anorthite and amorphous phase. At a higher temperature of 950 °C, anorthite decomposes to form a completely amorphous glassy phase

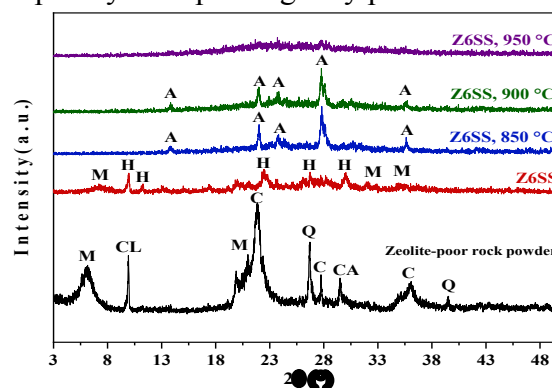


Figure 11. X-ray diffractogram of zeolite-poor rock, alkali-activated (ZS), and (Z6SS) foamed specimens fired at variable temperatures.

4.4.3. Micro-CT analysis of zeolite-poor rock/sawdust foams

In Fig. 12, ZS had both big and tiny pores with spherical-like structures. The inclusion of 6% sawdust powder in the Z6SS sample increases the pore sizes and leads to irregular pore shape formation (maze-like structure).

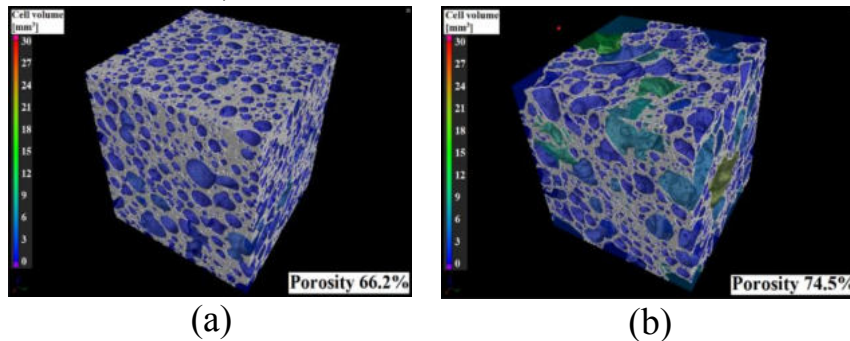


Figure 12. 3D CT scan images of a) of ZS, b) Z6SS

4.4.4. Technical properties of the fired zeolite-poor rock/sawdust foams

The densities of the samples tend to decrease with increasing the sawdust content and the sintering temperature. Upon increasing the sintering temperature, the alkali-activated samples transformed from solid to semi-liquid with relatively low viscosity, while the sawdust incorporated in the sample decomposed simultaneously, creating carbon dioxide. The rapid formation of the gas increased the internal pressure in the viscous mixture, causing it to expand increasing the porosity; therefore, the density, thermal conductivity and compressive strength decreased (Fig. 13).

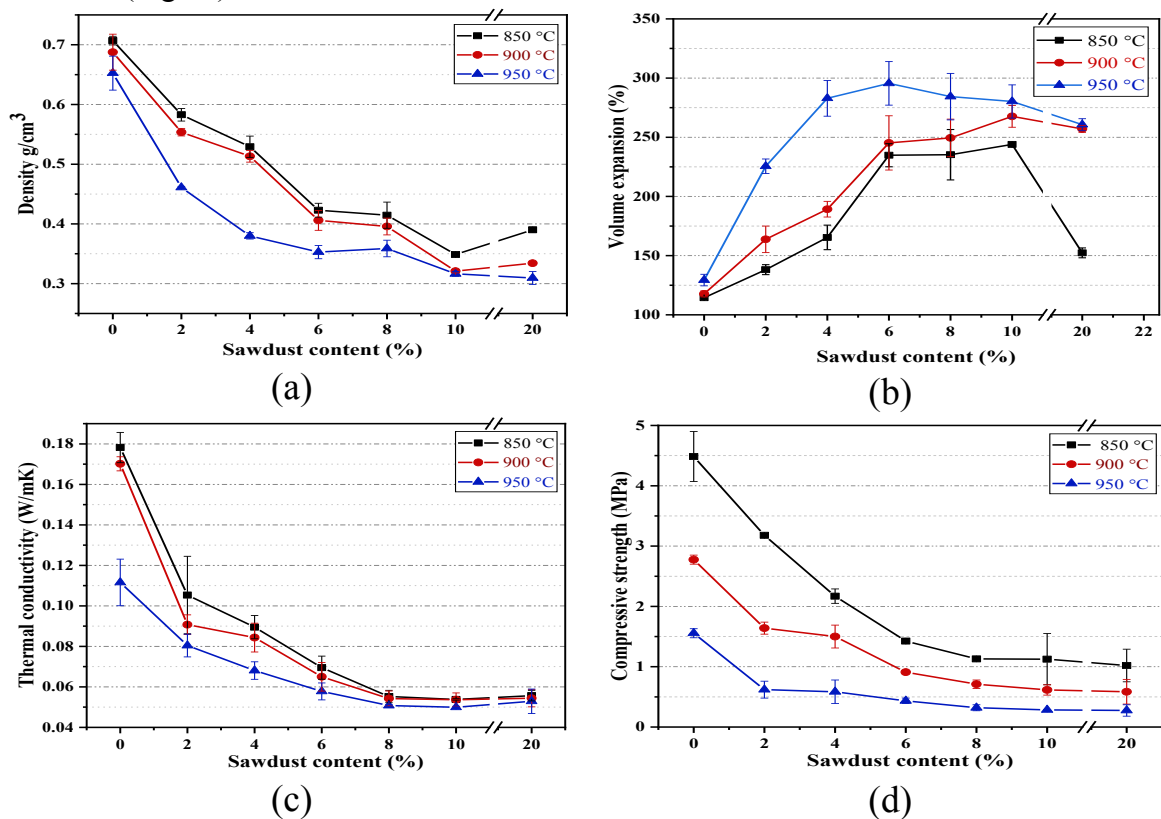


Figure 13. The correlation between a) density, b) apparent porosity c) thermal conductivity, d) and eggshell content of the samples sintered at different temperatures

4.5. Result of Innovative glass-ceramic foams based on zeolite-poor rocks incorporated eggshell

4.5.1. Dimensional properties of the sintered zeolite-poor rock/eggshell foams

Fig. 14 depicts the dimensional changes of the different zeolite-poor rock/eggshell foams burned at varying temperatures, acquired by images on a normal scale. It is worth highlighting that raising the amount of eggshell content first leads to a rise in pore size and total volume expansion, followed by shrinkage and reduced pore size. On the other hand, increasing the sintering temperature increases the pore size. This indicates the strong correlation between the pore size, amount of the foaming agent, and sintering temperature. The CaO acts as a flux reducing the melting temperature; therefore, a sparkling glassy phase is formed at high eggshell content and high sintering temperature. The reference samples (ZS) heat-treated at a temperature range of 850 °C show cracks in the surface due to insufficient molten-phase formation.



Figure 14. Photos of foamed samples with varied contents of eggshell sintered at different temperatures

4.5.2. Micro-CT analysis of zeolite-poor rock/eggshell foams

The overall porosity of the produced reference foams grew from 66.2 to 71.9% as the quantity of eggshell increased to 4% (Fig. 15). Moreover, the pore size also increased due to the higher amount of gas emitted.

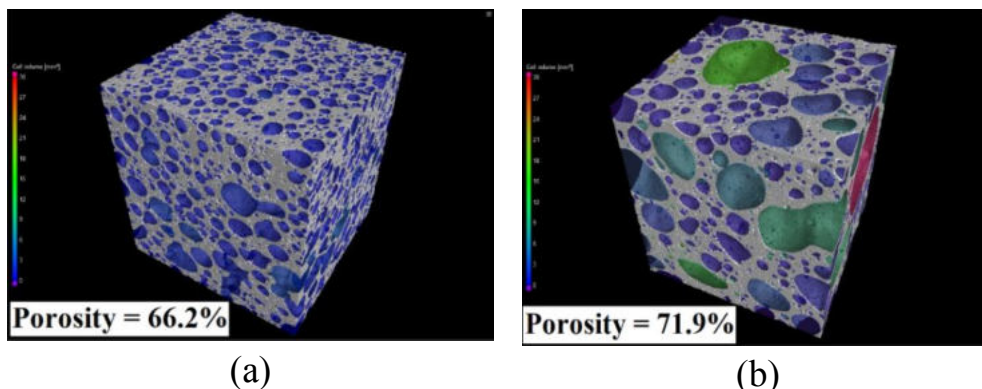


Figure 15. 3D CT scan images of a) of ZS, b) Z4ES

4.5.3. Technical properties of the fired zeolite-poor rock/eggshell foams

Fig. 16 depicts the influence of eggshell and sintering temperature on the properties of the foamed samples. As the eggshell content increases, the density, thermal conductivity and compressive strength of the specimens reduce until the addition of 4% eggshell. Then it starts to increase gradually with increasing the amount of eggshell. The reason for this process is that upon sintering, eggshell decomposes and produces CaO and CO₂. At lower eggshell content, the gas is entrapped in the high viscous phase leading to high blowing capability. However, at high eggshell content and sintering temperature, the produced CaO affects the viscosity of the molten glass phase and hinders the foaming behaviour resulting in lower foamability. Therefore, higher densification of the samples takes place.

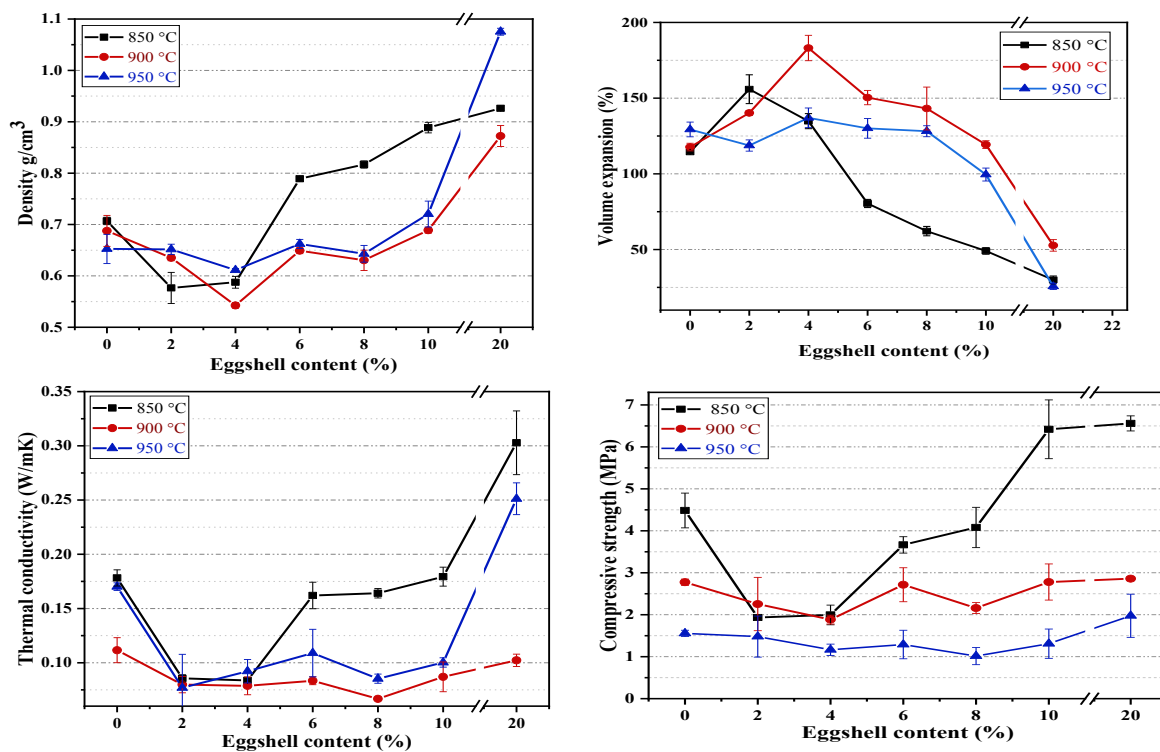


Figure 16. The correlation between a) density, b) apparent porosity c) thermal conductivity, d) and eggshell content of the samples sintered at different temperatures

5. Summary

The current study is the first work to investigate the usage of zeolite-poor rock and solid waste (sawdust and eggshell) in the manufacturing of innovative ceramic bricks and glass-ceramic foams with enhanced thermal insulation properties in an attempt to address the sustainability-connected challenges. Based on the experimental findings, the following conclusions can be obtained. Porous bricks and glass-ceramic foams based on zeolite-poor rock and solid waste (sawdust and eggshell) have been successfully prepared and characterised. The produced samples possess lightweight, good compressive strength and superior thermal insulation. The proper milling, compaction and sintering conditions have been determined. The alkali-activation process led to formation of low temperature-melting compound. The porous brick and glass-ceramic foams could be a potential candidate for thermal insulation materials in buildings.

6. Claims/New scientific results

Based on the integrated experimental research studies of ceramic bricks and glass-ceramic foams production from zeolite-poor rocks and solid waste (sawdust and eggshell), the following new scientific findings were derived:

6.1. Claims for the development of ceramic bricks

Claim 1. Preparation of innovative composite bricks based on zeolite-poor rock and solid waste (sawdust and eggshell)

It was proved that it is possible to produce innovative building bricks with low density (1.4–1.88 g/cm³) and low thermal conductivity (0.13–0.7 W/mk) based on zeolite-poor rock (Tokaj) ($D < 100 \mu\text{m}$) together with solid waste (sawdust and eggshell powder) ($D_{90} < 100 \mu\text{m}$). Sawdust and eggshell were added as a partial replacement for zeolite-poor rock in the specimens. The replacement percentages of sawdust and eggshell were 0–10 wt% and 0–20 wt%, respectively, by mass of zeolite-poor rock. The mixed powders were milled for 15 min at 150 rpm to produce homogenous mixtures. The prepared mixtures were pressed at 40–45 MPa. The produced green ceramic samples were then sintered at variable temperatures (950, 1050, 1150, and 1250 °C) for 3 h holding time and a heating rate of 60 °C/h. Bricks produced by this technique using these raw materials show no efflorescence (no salt formation on the surfaces).

Claim 2. The effect of sawdust and eggshell addition on the pores of the produced bricks.

I established that the inclusion of 8 wt% sawdust ($D_{90} < 100 \mu\text{m}$) into zeolite-poor rock powder ($D < 100 \mu\text{m}$) followed by ball milling for 15 min at 150 rpm, dry pressing at 45 MPa and sintering at a temperature range of 950–1250 °C with a residence time of 3 h and a heating rate of 60 °C/h resulted in bricks with an irregular porous structure having large numbers of open pores (Fig. A1). While the incorporation of 20 wt% eggshell powder ($D_{90} < 100 \mu\text{m}$) into the zeolite-poor rock powder, followed by the same production process with the same conditions, led to the formation of a cellular structure with a relatively larger number of round-like closed pores (Fig. A2).

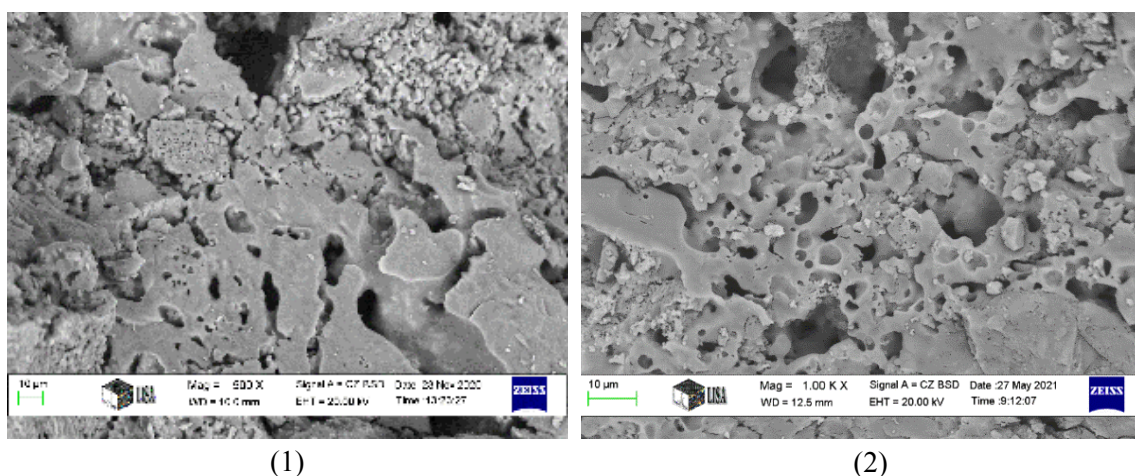


Fig. A. SEM images of the fracture surface of a) zeolite-poor rock and b) zeolite-poor rock+20% eggshell sintered at 1050 °C

Claim 3. The effect of eggshell addition on the compressive strength of the produced samples

I established that with the addition of 10 wt% eggshell powder ($D_{90} < 100 \mu\text{m}$) into zeolite-poor rock powder ($D < 100 \mu\text{m}$), followed by the ball milling, dry pressing at 45 MPa and sintering at a temperature range of 950-1250 °C with a residence time of 3 h and a heating rate of 60 °C/h, bricks with higher compressive strength can be obtained compared to the bricks containing the same amount of sawdust ($D_{90} < 100 \mu\text{m}$). This could be explained by the fact that during the sintering, the eggshell decomposes and produce CaO, which acts as a flux that induces the liquid phase formation causing verification that binds the particles together and results in higher compressive strength of the produced eggshell containing bricks (Fig. B2).

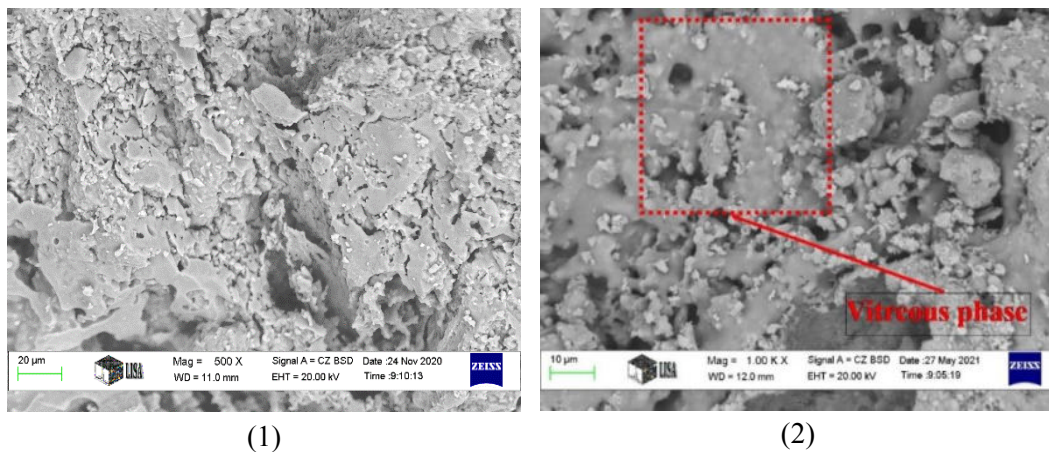


Fig. B. SEM images of (a) zeolite-poor rock + 6% sawdust (b) zeolite-poor rock + 10% eggshell samples sintered at 1050 °C showing the formation of the vitreous phase

Claim 4. Formation of mullite whisker in the composite bricks containing sawdust

I established that the inclusion of 8 wt% sawdust into zeolite-poor rock ($D < 100 \mu\text{m}$), followed by the ball milling for 15 min at 150 rpm, dry pressing at 45 MPa and sintering at a temperature range of 950-1250 °C with a residence time of 3 h, contributes to the firing raising the temperature. As a result, a mullite phase in a whisker-like structure has been formed at a relatively lower temperature (1150 °C), as confirmed by SEM, EDS (Fig. C) and XRD (Fig. D).

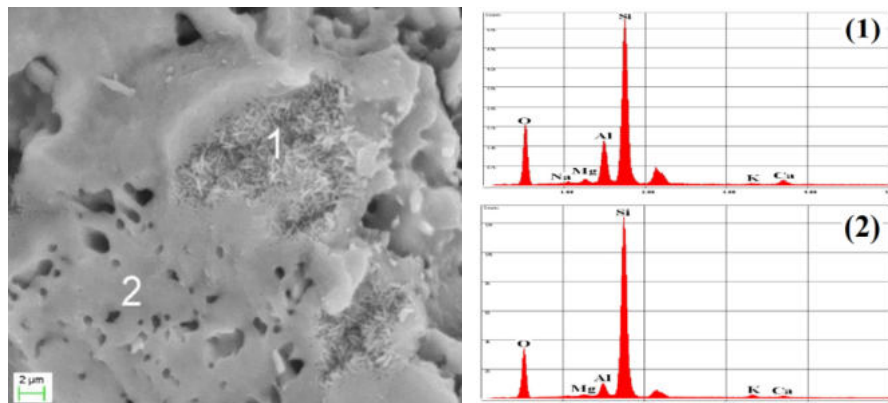


Fig. C. SEM and EDS micrograph of the fracture surface of zeolite + 8% sawdust sintered at 1150 °C

6.2 Claims for manufacturing of ceramic foams

Claim 5. Development of new glass-ceramic foams based on zeolite-poor rock and solid waste (sawdust and eggshell)

It was proved that it is possible to produce new glass-ceramic foams with low density ($0.3\text{--}1.07\text{ g/cm}^3$), low thermal conductivity ($0.04\text{--}0.3\text{ W/mk}$) and good compressive strength ($0.3\text{--}6.7\text{ MPa}$) based on zeolite-poor rock ($D < 100\ \mu\text{m}$) and (sawdust and eggshell powder) ($D_{90} < 100\ \mu\text{m}$) using alkali activation and reactive sintering techniques. Sawdust and eggshell partially substitute zeolite-poor rock. The substitution percentages were $0\text{--}20\%$ by wt% of zeolite-poor rock. The prepared powder mixtures were treated with 2M NaOH solutions for alkali activation, well-mixed for 5 min and then dried in the oven at $200\text{ }^\circ\text{C}$ for 2 days . The alkali-activated dried powders were ground in a planetary ball mill for 15 min at 150 rpm . Using uniaxial pressing machines at a pressure of 18 MPa , the milled powders were then compacted to form cylindrical pellets. The green ceramic bodies were heat-treated at varied temperatures ($850, 900, \text{ and } 950\text{ }^\circ\text{C}$) for 5 min holding time, with $5\text{ }^\circ\text{C/min}$ heating rate.

Claim 6. The alkali-activation modified the structure of the produced mixtures containing sawdust and eggshell

I established that the microstructure of the alkali-activated samples could be modified by the addition of sawdust and eggshell ($D_{90} < 100\ \mu\text{m}$). The alkali activation of milled zeolite-poor rock + $6\text{ wt}\%$ sawdust using 2M of NaOH followed by drying at $200\text{ }^\circ\text{C}$ for 2 days led to the formation of wickers-like aluminosilicate structure intergrowing through the thick matrix at sub-micron and nanoscale sizes (SEM images, Fig. E1). While in the case of the sample containing milled zeolite-poor rock + $4\text{ wt}\%$ eggshell, the alkali-activation in the same condition leads to the decomposition of zeolite-poor rock, followed by a chemical reaction, resulting in the formation of needle-like nanofibers intergrowing from a matrix (Fig. E2). The modification of these different nanostructures (large surface area) makes it possible to produce glass-ceramic foams at lower temperature ($850\text{--}950\text{ }^\circ\text{C}$) with different properties.

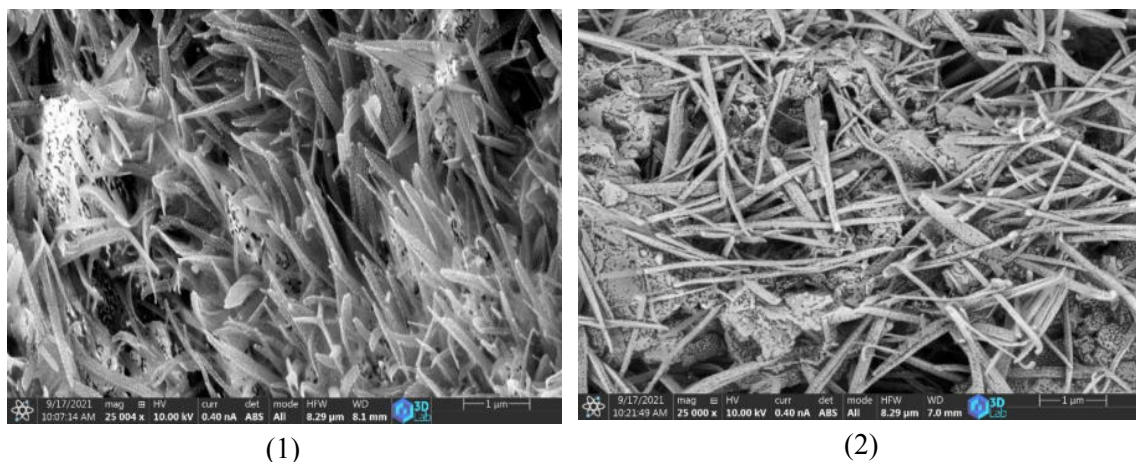


Fig. E. SEM images of the alkali-activated mixtures (zeolite-poor rock + 4% sawdust and zeolite-poor rock + 4% eggshell) at different magnifications

Claim 7. Development of zeolite-poor rock/sawdust foams with the lowest thermal conductivity.

I demonstrated that the application of 8 wt% of sawdust to zeolite-poor rock ($D_{90} < 100 \mu\text{m}$) followed by the alkali activation with 2M NaOH solutions, drying at 200 °C for 2 days and sintering at temperatures of 850 °C for 5 min holding time, with 5 °C/min heating rate, leads to the development of foams with the lowest thermal conductivity (0.04 W/mk) compared to the samples without sawdust (Fig. F) and (Fig. G).

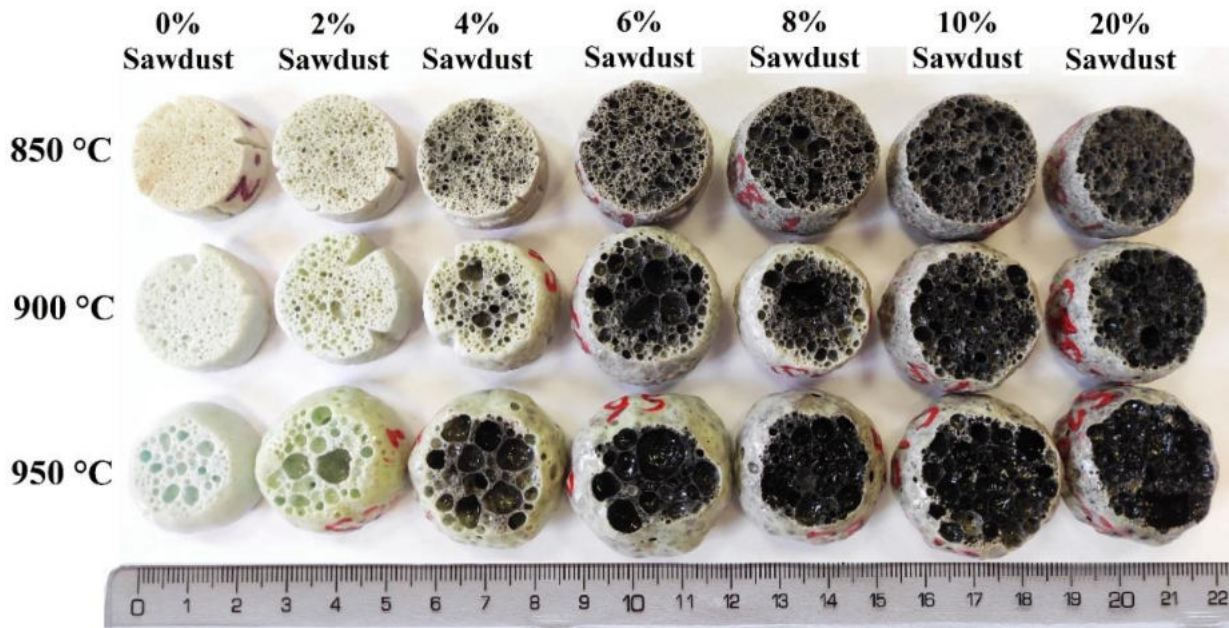


Fig. F. The produced foams with different sawdust content sintered at different temperature

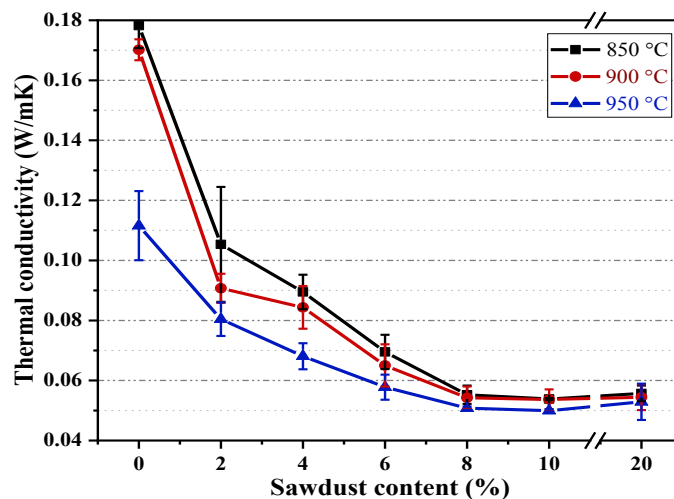


Fig. G. The correlation between thermal conductivity, and sawdust content of the samples sintered at different temperatures

Claim 8. The effect of the sawdust and eggshell incorporation on the foamability of the alkali-activated mixture.

I established that softening and foamability of the alkali-activated zeolite-poor rock (2M NaOH, 200 °C, 2 days) can be modified by using different foaming agents. In the case of alkali-activated zeolite-poor rock (D90<100 μm) containing sawdust (2-20 wt%) (D90<100 μm) sintered in the temperature range of 40-1200 °C, the foaming occurs in 3 steps reaching a maximum height of 216%, followed by a collapse of the foams (Fig. H). While in the case of alkali-activated zeolite-poor rock containing eggshell (2-20 wt%) (D90<100 μm) sintered in the temperature range of 40-1200 °C, the foaming process takes place in two stages showing a maximum expansion in the height of 188% (Fig. I). This change is due to the different behaviour of the decomposition of the foaming agents. During the sintering, the sawdust decomposition takes place in a temperature interval of 230–650 °C, while the eggshell decomposition occurs in the temperature range of 620–927 °C, producing gas that contributes to the foaming of the samples.

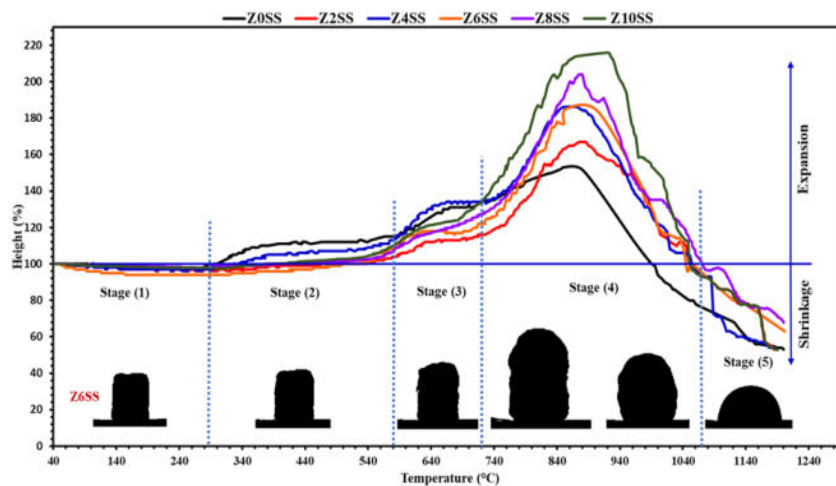


Fig. H. Heating microscope graphs of zeolite-containing sawdust samples heat-treated in the temperature range (40–1200 °C) at 10 °/min.

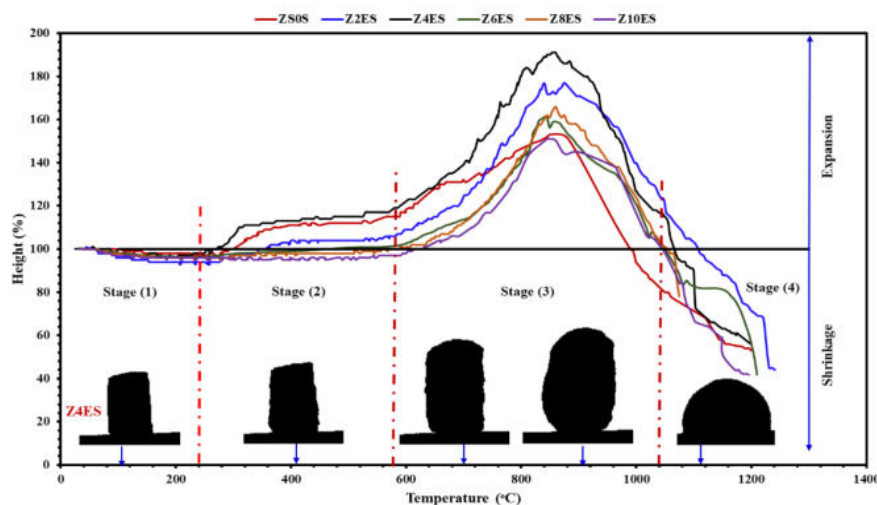


Fig. I. Heating microscope curves of different zeolite-poor rock/eggshell samples sintered in a temperature interval of (40-1200 °C) at 10 °/min

Claim 9. The effect of the sawdust and eggshell addition on the pore structure and compressive strength of the produced foams.

I established that by the addition of the sawdust and eggshell to alkali-activated zeolite-poor rock (2M NaOH, 200 °C, 2 days) sintered at 900 °C, the pore's structure can be modified, which influenced the compressive strength of the produced samples. The produced alkali-activated zeolite-poor rock foams sintered at 900 °C with a heating rate of 5 °C/min and residence time of 10 min possess spherical and small pore sizes with higher compressive strength (6.7 MPa) (Fig. J1), while the alkali-activated samples containing 4 wt% eggshells sintered at 900 °C with a heating rate of 5 °C/min and residence time of 10 min produce foams having spherical and large pores (Fig. J2) with a moderated compressive strength (1.4 MPa). However, the alkali-activated sample incorporated 6 wt% sawdust sintered at 900 °C with a heating rate of 5 °C/min and residence time of 10 min produced foams with irregular pore size and structure (Fig. J3) and exhibited the least compressive strength (2 MPa). The spherical shape of the pores and relatively better distribution are connected to the relatively high compressive strength in samples (reference and sample containing 4 wt% eggshells).

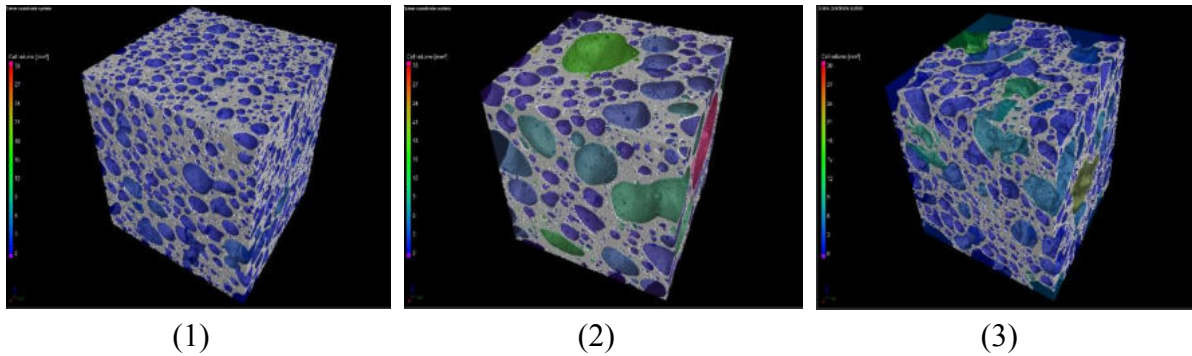


Fig. J. 3D image of 1) ZS, 2) Z4ES and 3) Z6SS

7. List of publications

- **Jamal Eldin FM Ibrahim**, Mohammed Tihtih, Emese Kurovics, László A. Gömze and István Kocserha. "Innovative glass-ceramic foams prepared by alkali activation and reactive sintering of zeolite-poor rock and sawdust for thermal insulation." *Journal of Building Engineering* (2022): **IF (7.144) D1**
- **Jamal Eldin FM Ibrahim**, László A. Gömze, Daniel Koncz-Horvath, Ádám Filep, and István Kocserha. "Preparation, characterisation, and physicochemical properties of glass-ceramic foams based on alkali-activation and sintering of zeolite-poor rock and eggshell." *Ceramics International* 48 (2022): 25905. **IF (5.532) Q1**
- **Jamal Eldin FM Ibrahim**, Mohammed Tihtih, and László A. Gömze. "Environmentally-friendly ceramic bricks made from zeolite-poor rock and sawdust." *Construction and Building Materials* 297 (2021): 123715. **IF (6.14) D1**
- **Jamal Eldin FM Ibrahim**, Olga B. Kotova, Shiyong Sun, Emese Kurovics, Mohammed Tihtih, and László A. Gömze. "Preparation of innovative eco-efficient composite bricks based on zeolite-poor rock and Hen's eggshell." *Journal of Building Engineering* 45 (2022): 103491. **IF (7.144) D1**
- **Jamal Eldin FM Ibrahim**, Emese Kurovics, Mohammed Tihtih, and László A. Gömze. "Ceramic bricks with enhanced thermal insulation produced from natural zeolite." *Pollack Periodica* 16, no. 3 (2021): 101-107. **IF (0.87) Q3**
- **Jamal Eldin FM Ibrahim**, Mohammed Tihtih, Emese Kurovics, Ethem İlhan Şahin László A. Gömze and István Kocserha. "Glass-ceramic foams produced from zeolite-poor rock (Tokaj)." *Pollack Periodica* 16, no. 3 (2021): 101-107. **IF (0.87) Q3**
- **Jamal Eldin FM Ibrahim**, Emese Kurovics, Mohammed Tihtih, and László A. Gömze and István Kocserha. "Synthesis and characterisation of alkali-activated zeolite-poor rocks." In *Journal of Physics: Conference Series*, vol. 2315, no. 1, p. 012020. IOP Publishing, 2022.
- **Jamal Eldin FM Ibrahim**, Kurovics, M. Tihtih, P. Somdee, A. G. Gerezgiher, K. Nuilek, E. E. Khine, and M. Sassi. "Preparation and Investigation of Alumina-Zeolite Composite Materials." In *Journal of Physics: Conference Series*, vol. 1527, no. 1, p. 012029. IOP Publishing, 2020. **IF (0.55) Q3**
- **Jamal Eldin FM Ibrahim**, and L. A. Gömze. "Investigation of the Rheological Properties of Complex Zeolite-Alumina Mixtures." In *Journal of Physics: Conference Series*, vol. 1527, no. 1, p. 012009. IOP Publishing, 2020. **IF (0.55) Q3**
- **Jamal Eldin FM Ibrahim**, Afanasy S. Apkarian, Mohammed Tihtih, Sergei N. Kulkov, and László A. Gömze. "In-situ carbonisation of natural zeolite-alumina composite materials incorporated sawdust." *Építőanyag-Journal of Silicate Based & Composite Materials* 73, no. 4 (2021). **IF (1.079)**
- **Jamal Eldin FM Ibrahim**, Dmitry A. Shushkov, Emese Kurovics, Mohammed Tihtih, Olga B. Kotova, Péter Pala, and László A. Gömze. "Effect of composition and sintering temperature on thermal properties of zeolite-alumina composite materials." *Építőanyag-Journal of Silicate Based & Composite Materials* 72, no. 4 (2020). **IF (1.079)**
- **Jamal Eldin FM Ibrahim**, Ayhan Mergen, Umut Parlak, Emese Kurovics, Mohammed Tihtih, and László A. Gömze. "Synthesis and characterisation of iron-doped GdMnO₃ multiferroic ceramics." *Építőanyag* (Online) 1 (2021): 24-27. **IF (1.079)**
- **Jamal Eldin FM Ibrahim**, Ayhen Mergen, Umut Parlak, and Emese Kurovics. "The Influence of Cr doping on the Structural and Magnetic Properties of HoMnO₃

Multiferroic Ceramics." In *IOP Conference Series: Materials Science and Engineering*, vol. 613, no. 1, p. 012009. IOP Publishing, 2019. **IF (0.51)**

- **Jamal Eldin FM Ibrahim**, L. A. Gömze. new zeolite-alumina composite materials-development and investigation, preparation of ceramic materials proceedings of the xiiith international conference, Jahodná, 25–27th June 2019. ISBN: 978-80-553-3314-4.
- **Jamal Eldin FM Ibrahim**, E. Kurovics, and L. A. Gömze. "Synthesis, characterisation and rheological properties of alumina-zeolite mixtures." *Multi Science-XXXIII. Micro CAD International Multidisciplinary Scientific Conference*, Hungary, [http://dx. doi. org/10.26649/musci](http://dx.doi.org/10.26649/musci), 2019
- **Jamal Eldin FM Ibrahim**, Ayhan Mergen, Ethem İlhan SAHİN, and Haythem S Basheer. "The effect of europium doping on the structural and magnetic properties of GdMnO₃ multiferroic ceramics." *Advanced Ceramics Progress* 3, no. 4 (2017): 1-5.

8. Acknowledgements

First and foremost, I would like to express my massive appreciation to my previous supervisor *Prof. László A. Gömze*, for his overwhelming support, advice, encouragement, commitment, and supervision right from the start till the midway of my Ph.D. candidature at University of Miskolc. *Prof. László A. Gömze* passed away in January 2022. He was a very dedicated and supportive person with a huge passion for research. My deepest appreciation goes to my current supervisor, *Dr. Kocserha István*, who has always been actively engaged in my Ph.D. project by guiding, inspiring, and supporting me. I would like to thank all the respected professors at the University of Miskolc who taught me various subjects over the first two years of the Ph.D. program. I also like to express my gratitude to the reviewer, *Prof. Dr. Péter Baumli*, for his insightful comments and suggestions on several aspects of my study. I would also like to extend my thanks to the reviewers, *Dr. Katalin Kopecskó* and *Dr. Péter Telek*, for their valuable feedback on my dissertation. I would also like to thank *Dr. Emese Kurovics* and *Mr. Gál Károly* for their unlimited support in the experimental work. My thanks extend to *Dr. Daniel Koncz-Horvath* for his assistance in conducting the investigation related to scanning electron microscopy and energy dispersive spectroscopy. I would also like to warmly thank *Dr. Róbert Géber* for his assistance in conducting the particle size distribution analysis. I owe thanks to *Dr. Andrea Simon* for her assistance in carrying out the thermal conductivity test. Many thanks to *Dr. Tamás Szabó* and *Ms. Ildikó Tasnádi* for their help with conducting FT-IR analysis. I would like to express my sincere gratitude to *Ms. Agnes Solczi* not only for being our faculty coordinator facilitating all the administrative work but also for her encouragement, support, and generous invitations to join her hiking trips. I also express my thankful feelings to my colleagues. I am thankful to all of them for the many hours of useful and enjoyable study, experimentation, and collaboration, as well as for sharing their extensive and valuable practical skills and knowledge with me. I would like to acknowledge Hungarian government for providing me full scholarship during the period of my Ph.D. study. I am very much thankful to Ministry of Higher Education, Sudan and University of Bahri for their financial support. Finally, my love and deep gratitude go to all my family members, who have always provided me with their unconditional love, encouragement, and deep support throughout my Ph.D. program and my academic career.

References

- [1] A. M. Omer, “Energy use and environmental impacts: A general review,” in *Advances in Energy Research*, vol. 17, no. 5, Nova Science Publishers, Inc., 2014, pp. 1–38.
- [2] X. Cao, X. Dai, and J. Liu, “Building energy-consumption status worldwide and the state-of-the-art technologies for zero-energy buildings during the past decade,” *Energy Build.*, vol. 128, pp. 198–213, Sep. 2016, [doi: 10.1016/j.enbuild.2016.06.089](https://doi.org/10.1016/j.enbuild.2016.06.089).
- [3] Johansson et al, “Global Energy Assessment [mdash] Toward a Sustainable Future.” pp. 1203–1306, 2012.
- [4] H. M. Taleb, “Using passive cooling strategies to improve thermal performance and reduce energy consumption of residential buildings in U.A.E. buildings,” *Front. Archit. Res.*, vol. 3, no. 2, pp. 154–165, Jun. 2014, [doi: 10.1016/j.foar.2014.01.002](https://doi.org/10.1016/j.foar.2014.01.002).
- [5] E. Clements-Croome, Derek, “Intelligent Buildings: An Introduction - 1st Edition - Derek Clements,” 2013. .
- [6] M. J. Munir, S. M. S. Kazmi, O. Gencel, M. R. Ahmad, and B. Chen, “Synergistic effect of rice husk, glass and marble sludges on the engineering characteristics of eco-friendly bricks,” *J. Build. Eng.*, vol. 42, no. March, p. 102484, 2021, [doi: 10.1016/j.jobe.2021.102484](https://doi.org/10.1016/j.jobe.2021.102484).
- [7] V. G. Karayannis, “Development of extruded and fired bricks with steel industry byproduct towards circular economy,” *J. Build. Eng.*, vol. 7, pp. 382–387, 2016, [doi: 10.1016/j.jobe.2016.08.003](https://doi.org/10.1016/j.jobe.2016.08.003).
- [8] J. J. Reinoso, A. C. Silva, F. Rubio-Marcos, S. R. H. Mello-Castanho, J. S. Moya, and J. F. Fernandez, “High chemical stability of stoneware tiles containing waste metals,” *J. Eur. Ceram. Soc.*, vol. 30, no. 14, pp. 2997–3004, 2010, [doi: 10.1016/j.jeurceramsoc.2010.02.017](https://doi.org/10.1016/j.jeurceramsoc.2010.02.017).
- [9] J. E. F. M. Ibrahim, O. B. Kotova, S. Sun, E. Kurovics, M. Tihtih, and L. A. Gömze, “Preparation of innovative eco-efficient composite bricks based on zeolite-poor rock and Hen’s eggshell,” *J. Build. Eng.*, vol. 45, 2022, [doi: 10.1016/j.jobe.2021.103491](https://doi.org/10.1016/j.jobe.2021.103491).
- [10] G. Marcari, G. Fabbrocino, and P. B. Lourenço, “Investigation on compressive behaviour of tuff masonry panels,” 2010.
- [11] D. Bozsaky, “The historical development of thermal insulation materials,” *Period. Polytech. Archit.*, vol. 41, no. 2, p. 49, 2010, [doi: 10.3311/pp.ar.2010-2.02](https://doi.org/10.3311/pp.ar.2010-2.02).
- [12] J. E. F. M. Ibrahim, E. Kurovics, M. Tihtih, and L. A. Gömze, “Ceramic bricks with enhanced thermal insulation produced from natural zeolite,” *Pollack Period.*, vol. 16, no. 3, pp. 101–107, 2021, [doi: 10.1556/606.2021.00341](https://doi.org/10.1556/606.2021.00341).
- [13] L. K. Kazantseva and S. V. Rashchenko, “Optimisation of porous heat-insulating ceramics manufacturing from zeolitic rocks,” *Ceram. Int.*, vol. 42, no. 16, pp. 19250–19256, 2016, [doi: 10.1016/j.ceramint.2016.09.091](https://doi.org/10.1016/j.ceramint.2016.09.091).
- [14] L. K. Kazantseva, T. S. Yusupov, T. Z. Lygina, L. G. Shumskaya, and D. S. Tsyplakov, “Foam glass from mechanoactivated zeolite-poor rock,” *Glas. Ceram. (English Transl. Steklo i Keramika)*, vol. 70, no. 9–10, pp. 360–364, Jan. 2014, [doi: 10.1007/s10717-014-9580-7](https://doi.org/10.1007/s10717-014-9580-7).
- [15] J. Tanijaya and D. Hardjito, “Experimental study on the use of natural zeolites as partial replacement for cement in concrete,” *EASEC-11 - Elev. East Asia-Pacific Conf. Struct. Eng. Constr.*, pp. 1–5, 2008.
- [16] Z. Chen, H. Wang, R. Ji, L. Liu, C. Cheeseman, and X. Wang, “Reuse of mineral wool waste and recycled glass in ceramic foams,” *Ceram. Int.*, vol. 45, no. 12, pp. 15057–15064, 2019, [doi: 10.1016/j.ceramint.2019.04.242](https://doi.org/10.1016/j.ceramint.2019.04.242).
- [17] J. Li et al., “Utilisation of coal fly ash from a Chinese power plant for manufacturing highly insulating foam glass: Implications of physical, mechanical properties and

- environmental features,” *Constr. Build. Mater.*, vol. 175, pp. 64–76, 2018, [doi: 10.1016/j.conbuildmat.2018.04.158](https://doi.org/10.1016/j.conbuildmat.2018.04.158).
- [18] T. Liu *et al.*, “Phase evolution, pore morphology and microstructure of glass ceramic foams derived from tailings wastes,” *Ceram. Int.*, vol. 44, no. 12, pp. 14393–14400, 2018, [doi: 10.1016/j.ceramint.2018.05.049](https://doi.org/10.1016/j.ceramint.2018.05.049).
- [19] J. Zhang, B. Liu, S. Zhao, H. Shen, J. Liu, and S. Zhang, “Preparation and characterisation of glass ceramic foams based on municipal solid waste incineration ashes using secondary aluminum ash as foaming agent,” *Constr. Build. Mater.*, vol. 262, p. 120781, 2020, [doi: 10.1016/j.conbuildmat.2020.120781](https://doi.org/10.1016/j.conbuildmat.2020.120781).
- [20] X. Ge, M. Zhou, H. Wang, L. Chen, X. Li, and X. Chen, “Effects of flux components on the properties and pore structure of ceramic foams produced from coal bottom ash,” *Ceram. Int.*, vol. 45, no. 9, pp. 12528–12534, 2019, [doi: 10.1016/j.ceramint.2019.03.190](https://doi.org/10.1016/j.ceramint.2019.03.190).